International Journal of Engineering & Technology, 7 (4) (2018) 5120-5126

International Journal of Engineering & Technology

Website: www.sciencepubco.com/index.php/IJET
doi: 10.14419/ijet.v7i4.26017
Research paper

Comparative study on viscosity and drag reducing performance between hydroxypropyl cellulose and hydroxypropyl cellulose-surfactant mixture

Ainoon Moreton-Shabirin [1] *, Hayder A Abdulbari [2]

[1] *Center of Excellence for Advanced Research in Fluid Flow, Universiti Malaysia Pahang, Gambang 26300, Kuantan, Pahang, Malaysia*
[2] *Faculty of Chemical and Natural Resources Engineering, Universiti Malaysia Pahang, Gambang 26300, Kuantan, Pahang, Malaysia*
**Corresponding author E-mail: hayder.bari@gmail.com*

Abstract

Ammonium Chloride (BZK) was found to enhance the drag reduction performance of a semi-rigid polymer Hydroxypropyl cellulose (HPC) in turbulent pipe flow. Rheology test showed that HPC's viscosity was higher than that of HPC-BZK mixture, and this showed that the presence of BZK had weakened the intermolecular strength of HPC molecules. Pressure-drop measurements indicated that HPC's and HPC-BZK mixture's drag reducing performance are (a) dependent on Reynolds number, and these mildly enhanced in the presence of BZK and (b) weakly dependent on additives concentration. Both HPC and HPC-BZK mixture showed a maximum drag reduction of 27% and 31%, respectively at Reynold's no. 59448 and gradual degradation thereafter. Although the presence of BZK enhanced the drag reduction performance of HPC in the mixture form, the experimental data indicated that BZK did not extend HPC's drag reduction performance nor assist the HPC to re-assume itself following structural degradation.

Keywords: *Drag reduction; Surfactant; Rigid Polymer.*

1. Introduction

For centuries, researchers have explored different techniques to minimize turbulent flow especially that within wall bounded areas such as the oil and gas pipeline. Known techniques include physical modification of the pipeline wall surface to incorporate riblets [1], oscillating walls or compliant surfaces [2], and addition of turbulent drag reducers such as suspended solids [3], [4], flexible polymer [5–8], and surfactants into the pipeline. These techniques aim to prevent and minimize the formation of turbulent eddies or drag which causes the turbulent flow. Of these techniques, using polymer drag reducers is found to be the most effective because a minute amount of the polymer is sufficient to produce > 50% of max drag reduction (DR) in the pipeline [9]. Examples of the common polymer drag reducers are polyethylene oxide (PEO), polyacrylamide (PAM) and polymethylmethacrylate (PAAM) [10]. These polymers are petroleum-based long chained and flexible polymer.

The explanation as to why flexible polymer makes an effective drag reducer was proposed by Lumley and Virk based on flexible polymer elongation and overall liquid viscosity, respectively [11], [12]. Lumley [11] suggested that at certain level of (Reynold's number) the flexible polymer molecule would elongate and unravel, and in so doing it would intervene in the formation of eddies which creates the turbulent flow. And Virk [12] proposed that the flexible polymer molecules positively interact with the solvent and this increases the overall liquid viscosity which stabilizes the turbulent boundary layer.

To enhance the drag reducing performance of a flexible polymer, surfactants are added to a water-soluble polymer to allow the former to interact strongly with the polymer hydrophobic groups which then leads to a strengthened association between polymer chains. As a result, this will produce an increased viscosity and then an increased drag reducing performance. Suksamranchit and Sirivat [13] reported that adding cationic surfactant to water soluble and flexible polymer PEO increased the overall viscosity and consequently increased the drag reducing performance of the PEO-cationic surfactant mixture. Matras et al [14] reported that adding cetyl trimethyl ammonium bromide (CTAB) with sodium salicylate (NaSal) salt to PEO also enhanced the drag reducing performance of the polymer, specifically in a straight pipeline. Kim et al. [15] tested the drag reduction performance of water soluble and flexible PAA-sodium dodecyl sulfate (SDS) mixture by using a rotating disk apparatus (RDA), and also found an enhanced drag reducing performance. These studies proved that in the presence of surfactant, the overall polymer drag reducing performance is enhanced and extended longer – before the polymer eventually goes through a permanent structural degradation.

On contrary, discussions on a surfactant's impact on rigid or semi-rigid polymer have not been sufficiently documented. Rigid and semi-rigid polymers are usually bio-based additives which are suitably used to facilitate pipe flow of various aqueous solutions. Kim et al. [16] and A. Japper-Jaafer [17] initiated a separate study to investigate the drag reducing performance of semi-rigid xanthan gum and rigid scleroglucan, respectively. Kim et al. observed that xanthan gum demonstrated a longer drag reducing performance in a rotating disk apparatus before it eventually degraded. A. Japper-Jaafar et al. found that scleroglucan showed a low level of drag reducing performance and suggested that it behaved similar to a flexible polymer carboxymethyl cellulose. But to-date, there have been no subsequent studies on enhancing and extending the rigid

or semi-rigid polymer's drag reducing performance through using surfactants. Additionally, the molecules which composed rigid or semi-rigid polymer have a restricted movement, and there have not been many discussions on either the semi rigid/rigid polymer-surfactant interaction or the semi rigid/rigid polymer-solvent interaction.

The present study thus aims to investigate the viscosity and drag reducing performances of a semi-rigid polymer hydroxypropyl cellulose (HPC) in turbulent pipe flow. HPC is a water soluble ether derivative of cellulose which can be obtained from wood, plant, bacteria, and algae. Cellulose is deemed an inexhaustible source of raw material [18]. Next, we will compare the viscosity data and drag reducing performances between that of HPC and HPC-surfactant mixture. Specifically, we will use a common cationic surfactant Benzyldimethylhexadecyl-Ammonium Chloride (BZK).

Your goal is to simulate the usual appearance of papers in the. We are requesting that you follow these guidelines as closely as possible.

2. Methodology

2.1. Materials

HPC is a white powder with an average molecular weight (MW) ~1,000,000 g/ mole, and its chemical formula is $(C_{12}O_{10}R_6)_n$. HPC is a non-ionic polymer. In contrast with a linear and flexible polymer, HPC is a branched polymer with semi-rigid polymer chain [19]. HPC and purchased from Sigma Aldrich. HPC is sued without any pre-treatment. Figure 1 below shows the chemical structure of HPC [20].

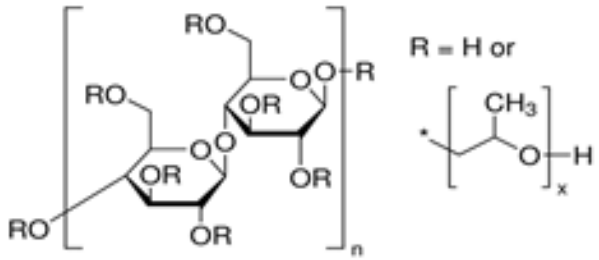

Fig. 1: Chemical Structure of HPC.

Figure 2 illustrates the chemical structure of BZK with a linear chemical formula of CH_3 $(CH_2)15N$ (Cl) $(CH_3)_2CH_2C_6H_5$. BZK is a cationic surfactant, highly water soluble and in the form of white solids with an average molecular weight (MW) ~ 396.09 g/mol. It is a widely used preservative often found in ophthalmic solutions and contact lens solutions. BZK is purchased from Sigma Aldrich and is used in this work as received without any pre-treatment.

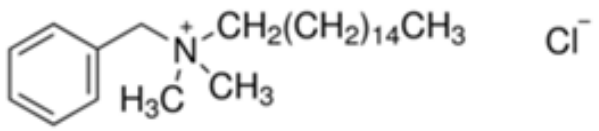

Fig. 2: Chemical Structure of BZK.

2.2. Transporting liquid

The transporting liquid used is water, and all additives solutions are readily soluble in water.

2.3. Sample preparation

HPC and BZK are water soluble and thus will be prepared as solutions to be added directly in aqueous pipe flow. Each additive concentration will be determined in weight parts per million (ppm) according to the weight/ weight basis. The additives are weighed to prepare 200ppm, 300ppm, 500ppm. 800ppm and 1000ppm of DRA solutions in water.

The DRA solution is prepared by dissolving the measured weight of the additive in distilled water with stirring using a magnetic stirrer for 1 hour. For both viscosity measurement and pipeline testing, the prepared DRA solution is left for 24 hours to allow thorough mixing.

2.4. Viscosity analysis

To examine viscosity, the DRA samples will be examined by a rheometer at Center of Excellence for Advanced Research in Fluid Flow (CARIFF), UMP. The rheometer equipment is Malvern Kinexus Lab+ series which is a rotational rheometer system that applies controlled shear deformation to a sample under test, to enable measurement of flow properties (such as shear viscosity and shear stress).

2.4. Experimental set up

The pipe loop constructed for the present work is illustrated below. It is a closed liquid circulation system to simulate a commercial pipeline system. The pipe loop will be used to investigate the drag reduction efficiencies for all DRA solutions. Basically, the pipe loop consists of a reservoir tank, pump, pipes, flow meters, and pressure drop sensors/gauges. All is built and integrated into one system to render its maximum flexibility during the operation.

The system comprises a stainless steel storage tank (0.6 m length x 0.35 m width x 0.5 m depth) with a total volume of 100 Ls. This tank is linked to a 0.025 m pipe diameter that is connected to a T-joint that will separate into two sections. The first section returns back to the main tank and supported with a ball valve. This pipe is used to control the flow rate in the main testing section. The second section serves as the start of the pressure drop and drag reduction testing section where the pipe will extend to 5 meters and then linked through two elbows to create a returning pipeline section as shown below. This provides a fully developed turbulent flow before entering the testing sections because the minimum length required for non-Newtonian solutions is 100X D. In the present work, it is 2.5m while the actual length is 5 m.

The testing section is divided into four pressure drop measurement sections wherein each is 1 m long. Each measurement section is connected to two pressure taps that are used to measure the pressure drop across the 1 m pipe as shown below. The pipeline system links back to the main tank thus forming a closed loop liquid circulation system.

A differential pressure transmitter (DPT-301) is used to measure the pressure drop across each testing section. The transmitter pressure drop measurement scales up to 6 bar. Additionally, a Burket 8035 minisonic flow meter is placed 1 meter away from the T-joint to ensure a minimum disturbance to the expected fully formed turbulent flow in each pressure drop measurement section.

All the data (pressure drop and flow rates) is conveyed online through a custom-made interface to a SCADA system that is specifically designed for the pipe loop. The SCADA system enables the user to record and save the flowrate and pressure drop reading against time.

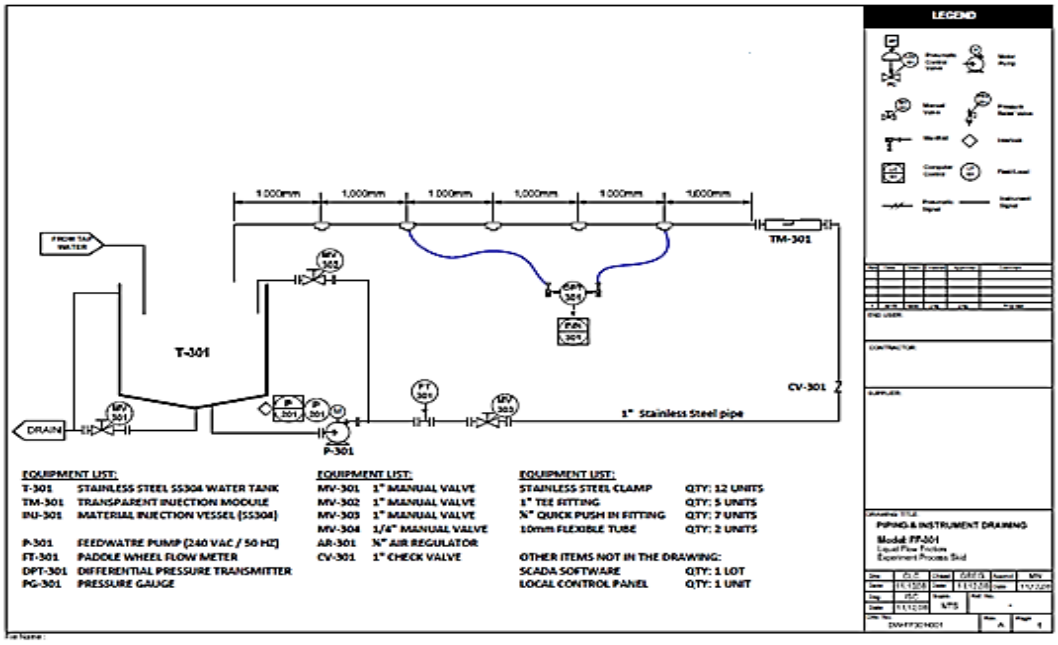

Fig. 1: Schematic Diagram of the Pipe Loop System.

2.5. Percentage drag reduction (%DR)

As water will be used as the transporting liquid, it will therefore be used as a reference point. Each time water is tested in the pipeline, the water pressure drop and torque readings will be observed and recorded. For the pipe flow, the pressure drop readings for the pure water (before DRA is added) at each flow rate will be recorded as ΔPb and the pressure drop readings (after DRA will be added) will be recorded as ΔPa.
The percentage drag reduction (%DR) will be calculated using the following equation:

$$\% \text{ Dr} = \frac{\Delta P_b - \Delta P_a}{\Delta P_b} \quad (1)$$

Where:
%DR = percentage drag reduction
ΔPb = pressure drop before drag reducer addition (mbar)
ΔPa = pressure drop after drag reducer addition (mbar)
Velocity (v) and Reynolds Number (Re) were calculated using the flow rate readings (Q), density (ρ), velocity (μ) and pipe diameter (d), for each run as follows:

$$\text{Re} = \frac{\rho * u * D}{\mu} \quad (2)$$

Where:
Re =Reynolds number (dimensionless)
ρ = density of the fluid, 1000 (kg/m3)
μ = viscosity of the fluid = 0.001 n.sec / m2 (c.p)
D = pipe diameter (0.025 m)
u = velocity of the fluid. m / sec

$$u = \frac{Q}{A} \quad (3)$$

Where:
Q = the volumetric flow rate m3/hr
A = cross sectional area (m2)

$$A = \frac{\pi}{4} D^2 \quad (4)$$

3. Result and discussions

3.1. Viscosity

The plot of shear viscosity against shear rate for HPC as shown in Figure 4 showed an increased dependence of the shear viscosity on shear rate with increasing concentrations (200ppm, 300ppm, 500ppm, 800ppm and 1000ppm). This plot agreed with the general shape for shear-thinning liquids.

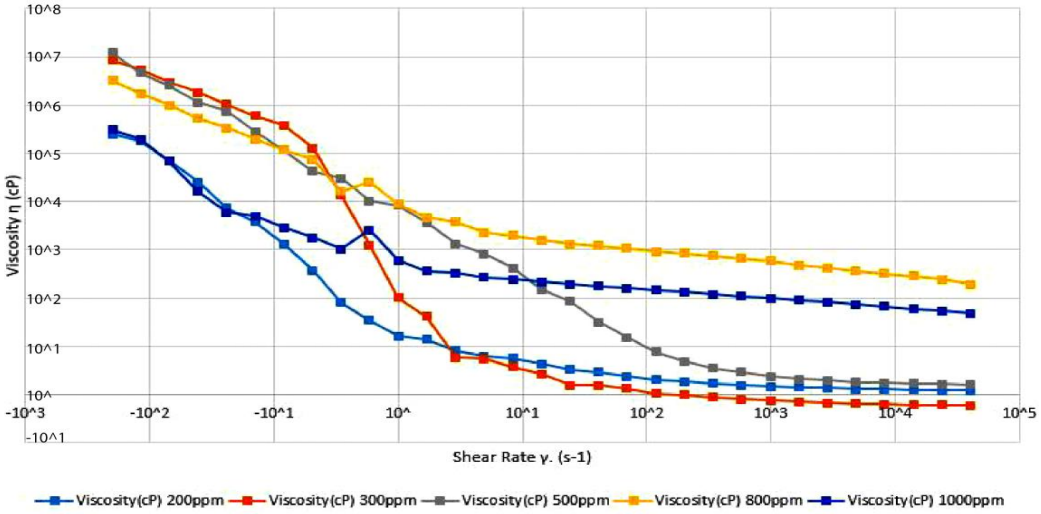

Fig. 2: HPC's Shear Viscosity vs. Shear Rate.

Viscosity was highest in the beginning and as the shear rate increased, viscosity decreased gradually to a constant lower value at higher shear rates, referred as the 'higher Newtonian region' or the 'second Newtonian region'. As observed, all HPC concentrations exhibited a high viscosity in the beginning when the shear rate was at minimum. The behavior of all concentrations seemed uniform i.e. showing the gradual breakdown of the viscosity under stress, and this plot shape confirms HPC's non-Newtonian behavior as a shear thinning liquid.

The plot of shear viscosity against shear rate for HPC-BZK mixture shown in Figure 5 showed an increased dependence of the shear viscosity on shear rate with increasing concentrations (200-200ppm, 300-300ppm, 500-500ppm, 800-800ppm and 1000-1000ppm). This plot agreed with the general shape for shear-thinning liquids.

In Figure 5, viscosity was highest in the beginning with the HPC-BZK mixture (1000ppm-1000ppm) leading, and as the shear rate increased viscosity decreased gradually to a lower value at higher shear rates. All HPC-BZK mixture concentrations exhibited a high viscosity in the beginning when the shear rate was at minimum. The behaviour of all concentrations seemed uniform i.e. showing the gradual breakdown of the viscosity under stress.

Figure 6 showed that HPC (800ppm) has a substantially higher viscosity than HPC-BZK Mixture (800ppm-800ppm). This implied that the intermolecular forces of HPC are weakened by the presence of BZK when HPC-BZK mixture is formed. Figure 7 compares the shear viscosities between 1000ppm HPC, 1000ppm BZK and 1000-1000ppm HPC-BZK. The viscosity of 1000ppm HPC was still higher than 1000-1000ppm HPC-BZK mixture. At extreme shear rates, however, HPC showed that its viscosity is much higher than HPC-BZK.

At both concentrations, HPC has a higher viscosity than that of HPC-BZK mixture. This implied HPC has a stronger intermolecular force compared to its mixture form, and thus the presence of BZK had weakened these forces in the mixture.

Viscosity reduction observed with HPC in the presence of BZK is usually encountered with a crude oil viscosity reducer. Generally, when a viscosity reducer molecule are introduced to a polymer, they would penetrate into the polymer and alter the intermolecular structure to the extent that the polymer is unable to form any bonding with either its own or other molecules. This created the over-dissolution of the polymer in the presence of the viscosity reducer molecules.

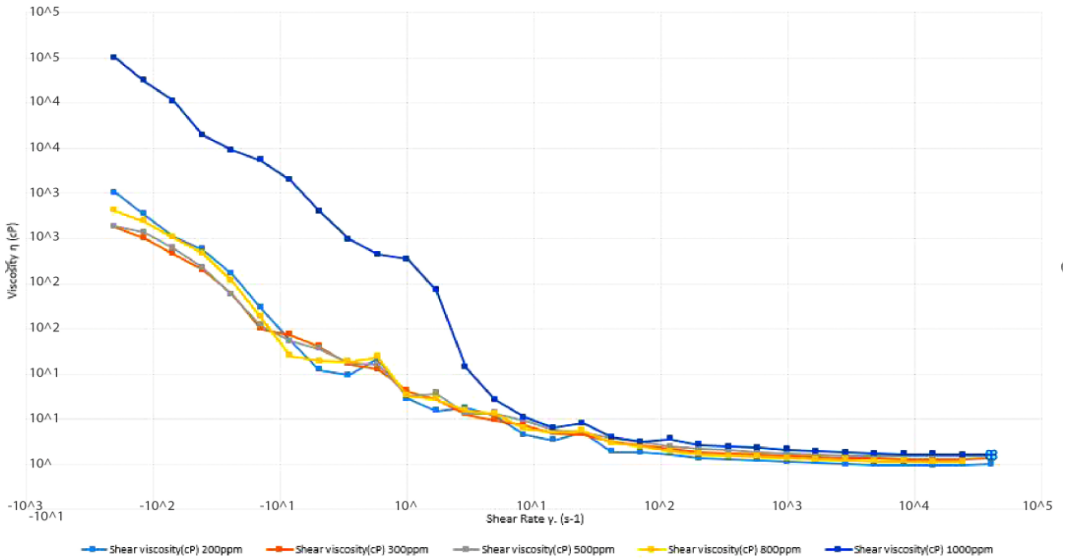

Fig. 3: HPC-BZK Mixture's Shear Viscosity V. Shear Rate.

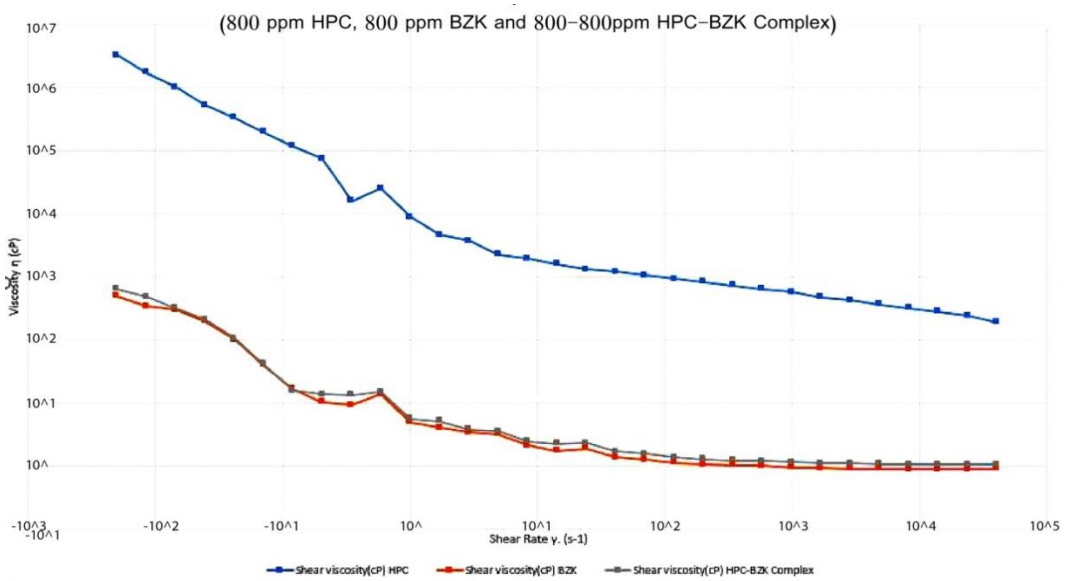

Fig. 4: Comparison on Viscosity between 800ppm HPC and 800-800ppm HPC-BZK Mixture.

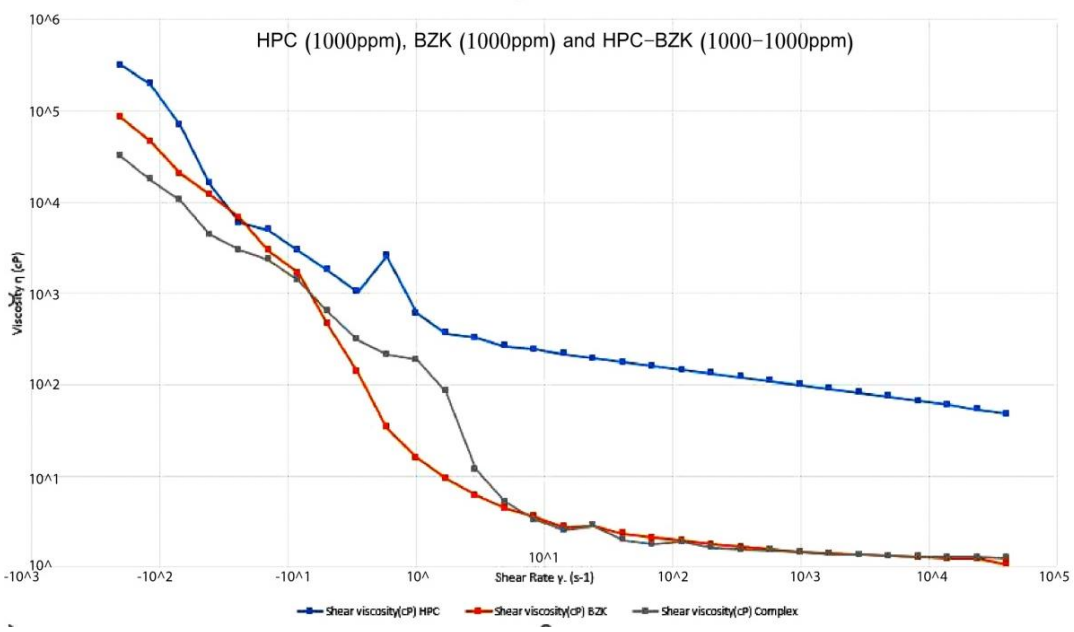

Fig. 5: Comparison on Viscosity between 1000ppm HPC and 1000-1000ppm HPC-BZK Mixture.

3.2. Pressure drop

3.2.1. Effect of Reynolds numbers

%DR of 1000ppm HPC, 1000 ppm BZK and 1000-1000ppm HPC-BZK mixture are plotted against different Reynolds numbers Re through a 1m pipe loop, in Figure 8. The degree of drag reductions for HPC and HPC-BZK mixture appeared to be mildly dependent on Reynolds Number. Most notably, HPC-BZK mixture showed higher maximum drag reduction (30.8%) than HPC (27.2%) specifically at Re: 59448.

%DR of 1000ppm HPC, 1000 ppm BZK and 1000-1000ppm HPC-BZK mixture are plotted against different Reynolds numbers Re through a 3m pipe loop, in Fig 9. The degree of drag reductions for HPC and HPC-BZK mixture appeared to be mildly dependent on Reynolds Number. Most notably, HPC-BZK mixture showed higher maximum drag reduction (30.3%) than HPC (23.9%) specifically at Re: 59448.

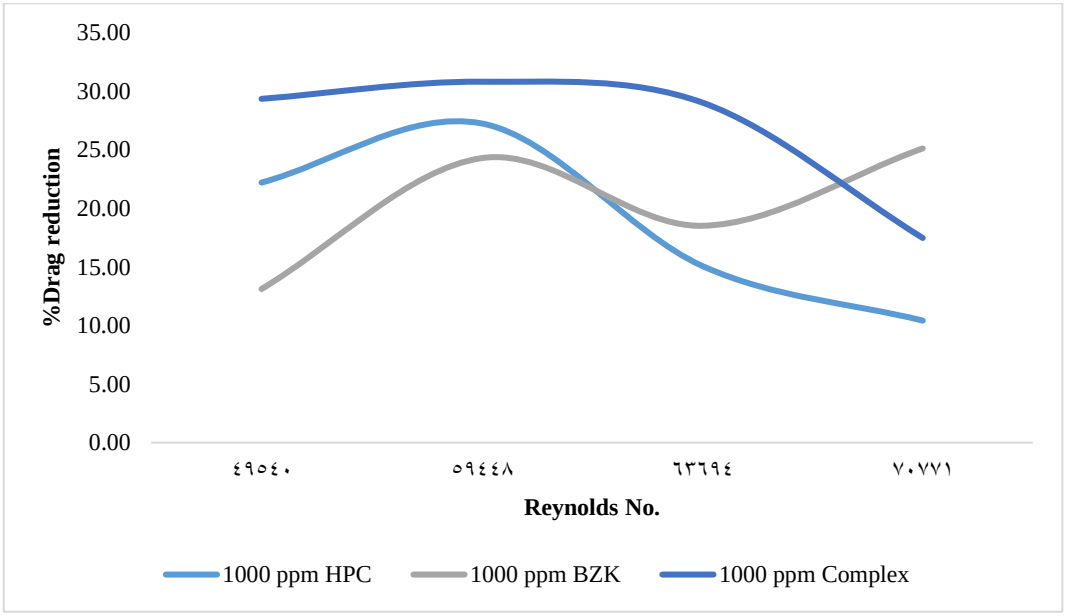

Fig. 6: %DR of HPC, BZK & HPC-BZK Mixture – 1 m Pipe Loop.

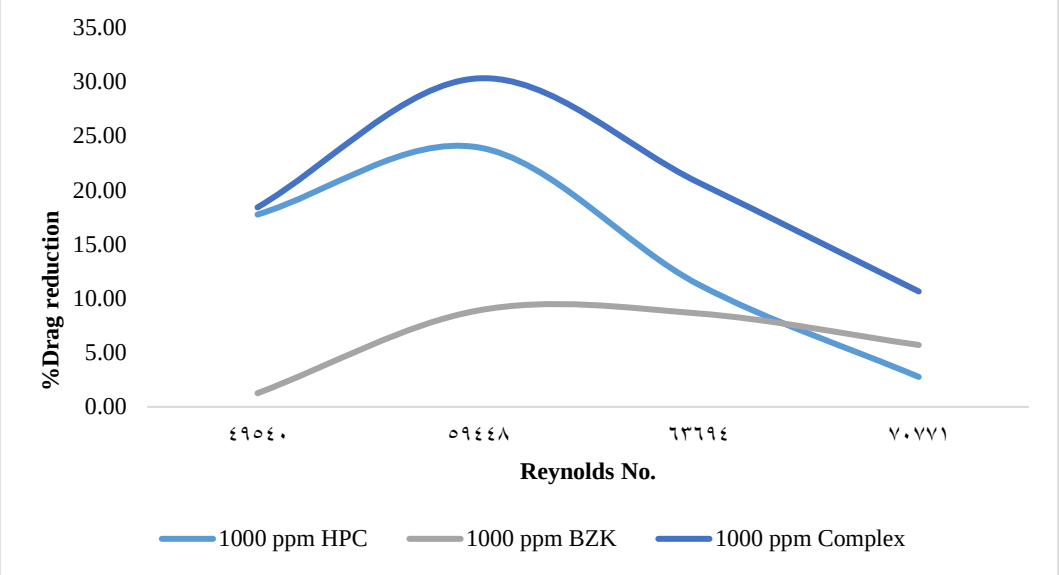

Fig. 7: %DR of HPC, BZK & HPC-BZK Mixture – 3 m Pipe Loop.

In both 1m and 3m, after the maximum drag reduction, both HPC and HPC-BZK mixture showed a gradual decline in drag reduction which marked the structural degradation of HPC. It is noted that HPC-BZK drag reduction decline did not seem to fluctuate, unlike what was anticipated based on BZK's drag reducing performance. This indicated that whilst BZK indeed enhanced HPC's drag reduction performance in the mixture form, BZK did not enable HPC to extend or lengthen its drag reduction performance longer.

3.2.2. Effect of concentration

%DR of HPC, BZK and HPC-BZK mixture are plotted against different concentrations (200-1000ppm) through a 1m pipe loop at Re:59448, in Figure 10. The figure indicated that for both HPC and HPC-BZK mixture, the drag reduction is weakly dependent on concentration. Increasing the concentration from 200ppm to 1000ppm saw a fluctuation where the drag reduction was high at 300ppm and low at 500ppm. Nevertheless, it was noted that the % drag reduction of HPC-BZK mixture was higher than that of HPC.

%DR of HPC, BZK and HPC-BZK mixture are plotted against different concentrations (200-1000ppm) through a 3m pipe loop at Re:59448, in Figure 11. The figure indicated that for both HPC and HPC-BZK mixture, the drag reduction is weakly dependent on concentration. Increasing the concentration from 200ppm to 800ppm saw an increase in the drag reduction. It however proves that the % drag reduction of HPC-BZK mixture was higher than that of HPC throughout the pipe loop experiment.

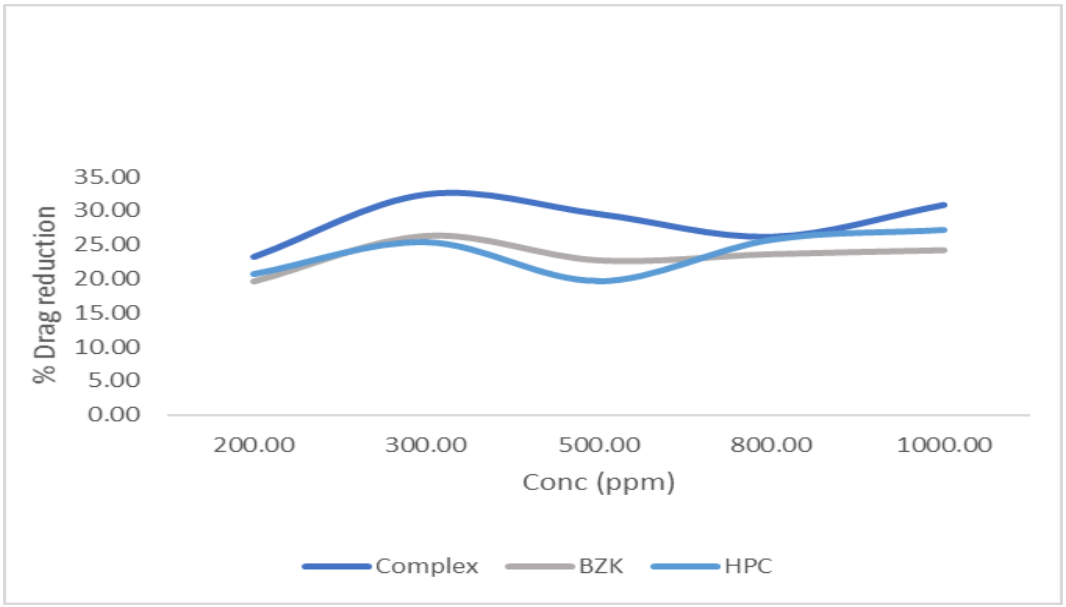

Fig. 8: %DR of HPC, BZK & HPC-BZK Mixture – 1 M Pipe Loop, Re: 59448.

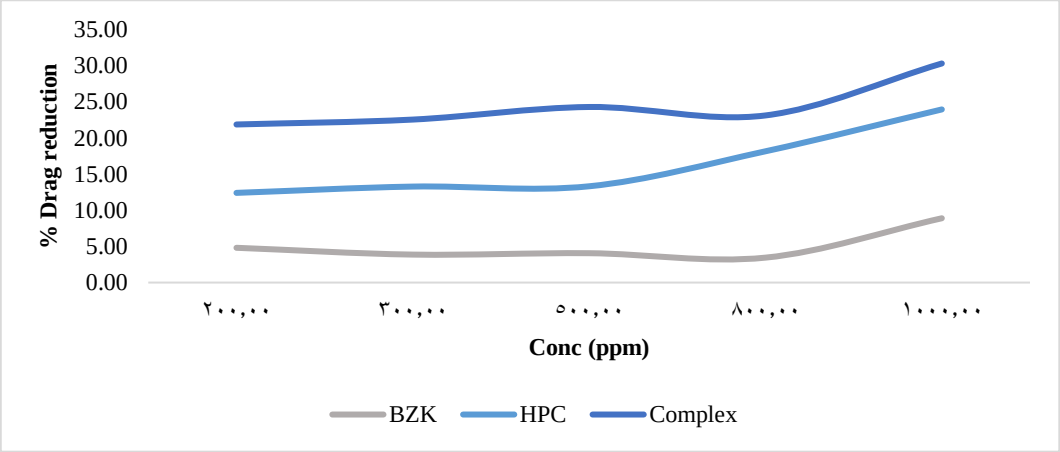

Fig. 9: %DR of HPC, BZK & HPC-BZK Mixture – 3 M Pipe Loop, Re: 59448.

Finally, given HPC's viscosity is higher than that of HPC-BZK mixture, and that subsequent pressure drop measurements indicated that HPC-BZK's mixture produced higher drag reducing performance than HPC; it was not able to be ascertained at this juncture if the drag reducing mechanism could be explained through viscosity per Virk's theory.

4. Conclusion

This study verified the drag reducing performance of semi-rigid polymer specifically hydroxypropyl cellulose (HPC) which was enhanced when a cationic surfactant Benzyldimethylhexadecyl-Ammonium Chloride (BZK) was added. The study also found that the viscosity of HPC was higher than that of HPC-BZK mixture, and this suggested that the presence of BZK surfactants had weakened the HPC intermolecular strength in the mixture. Although HPC-BZK mixture produced a higher drag reduction performance, the drag reducing pattern between HPC and HPC-BZK mixture is similar in that both reached a maximum drag reduction and followed by a structural degradation. This suggested that while BZK enhanced the HPC's drag reduction performance, it did not extend or lengthen its drag reduction performance. No fluctuation was observed in the drag reducing performance after the maximum drag reduction occurred and this suggested the absence of free micelles that could enable the structurally impacted HPC to reassume its structure in order to retain its drag reduction performance. In this respect, a surfactant's interaction with a semi-rigid polymer, in our case HPC, is not similar to that of a flexible polymer-surfactants interaction. It is therefore suggested that in order to fully elucidate the semi rigid polymer-surfactant's interaction, one will require the use of multiple tools such as optical microscopy, cryo-TEM, AFM, and NMR.

Acknowledgement

This work benefited from the support of Universiti Malaysia Pahang, Gambang 26300, Kuantan, Pahang, Malaysia.

References

[1] Abdulbari HA, Mahammed HD, Yaacob ZB & Mahmood WK (2016), Shark skin for enhancing the flow of underwater vehicles. *ARPN J Eng Appl Sci*, 16, 9895–900.

[2] Abdulbari HA, Yunus RM, Abdurahman NH & Charles A (2013), Going against the flow-A review of non-additive means of drag reduction. *Journal of Industrial and Engineering Chemistry*, 19, 27–36. https://doi.org/10.1016/j.jiec.2012.07.023.

[3] Abdulbari HA & Yue KK (2011), Studying the effect of magnetic force on increasing the drag reduction performance of suspended solids on the turbulent flow in pipelines: An experimental approach. *Int J Environ Sci Dev*, 4, 264–7. https://doi.org/10.7763/IJESD.2011.V2.135.

[4] Abdulbari HA, Nour AH, Kor K & Abdalla AN (2011), Investigating the effect of solid particle addition on the turbulent multiphase flow in pipelines. *Int J Phys Sci*, 15, 3672–9.

[5] Abdulbari HA, Shabirin A & Abdurrahman HN (2014), Biopolymers for improving liquid flow in pipelines—A review and future work opportunities. *J Ind Eng Chem*, 4, 1157–70. https://doi.org/10.1016/j.jiec.2013.07.050.

[6] Abdulbari HA, Letchmanan K & Yunus RM (2011), Drag reduction characteristics using aloe vera natural mucilage: An experimental study. *J Appl Sci*, 1039–43.

[7] Akindoyo EO, Abdulbari HA & Yousif Z (2015), A dual mechanism of the drag reduction by rigid polymers and cationic surfactant: Complex and nanofluids of xanthan gum and hexadecyl trimethyl ammonium chloride. *Int J Res Eng Technol*, 2, 84–93.

[8] Abdulbari HA, Kamarulizam HS & Nour AH (2012), grafted natural polymer as new drag reducing agent: An experimental approach. *Chem Ind Chem Eng Q*, 361–71. https://doi.org/10.2298/CICEQ111206012A.

[9] Rollin B, Dubief Y & Doering CR (2011), Variations on Kolmogorov flow: turbulent energy dissipation and mean flow profiles. *J Fluid Mech*, 204–13. https://doi.org/10.1017/S0022112010006294.

[10] Virk PS (1975), turbulent kinetic energy profile during drag reduction. *Phys Fluids*, vol. 4, pp.415–9. https://doi.org/10.1063/1.861166.

[11] Lumley JL (1973), Drag reduction in turbulent flow by polymer additives. *J Polym Sci Macromol Rev*, 1, 263–90. https://doi.org/10.1002/pol.1973.230070104.

[12] Virk PS (1975), Drag reduction fundamentals. *AIChE Journal*, 21, 625–56. https://doi.org/10.1002/aic.690210402.

[13] Suksamranchit S, Sirivat A & AJamieson AM (2006), Polymer-surfactant complex formation and its effect on turbulent wall shear stress. *J Colloid Interface Sci*, 1, 212–21. https://doi.org/10.1016/j.jcis.2005.07.001.

[14] Matras Z, Malcher T & Gzyl-Malcher B (2008), the influence of polymer-surfactant aggregates on drag reduction. *Thin Solid Films*. 24, 8848–51. https://doi.org/10.1016/j.tsf.2007.11.057.

[15] Kim JT, Kim CA, Zhang K, Jang CH & Choi HJ (2011), Effect of polymer-surfactant interaction on its turbulent drag reduction. *Colloids Surfaces A Physicochem Eng Asp*, 1-3, 125–9. https://doi.org/10.1016/j.colsurfa.2011.04.018.

[16] Kim CA, Jo DS, Choi HJ, Kim CB & Jhon MS (2000), A high-precision rotating disk apparatus for drag reduction characterization. *Polym Test*, 1, 43–8. https://doi.org/10.1016/S0142-9418(99)00077-X.

[17] Japper-Jaafar A, Escudier M &, Poole RJ (2009), turbulent pipe flow of a drag-reducing rigid "rod-like" polymer solution. *J Nonnewton Fluid Mech*, 1-3, 86–93. https://doi.org/10.1016/j.jnnfm.2009.04.008.

[18] Singh RP, Karmakar GP, Rath SK, Karmakar NC, Pandey SR & Tripathy T (2000), Biodegradable drag reducing agents and flocculants based on polysaccharides: Materials and applications. *Polym Eng Sci*, 1, 46–60. https://doi.org/10.1002/pen.11138.

[19] Kabir M & Reo J (2009), Hydroxypropyl Cellulose. *Handb Pharm Excipients*, 317–22.

[20] Martins RM, Da Silva CA, Becker CM, Samios D, Christoff M & Bica CID (2006), Anionic surfactant aggregation with (hydroxypropyl) cellulose in the presence of added salt. *J Braz Chem Soc*, 5, 944–53. https://doi.org/10.1590/S0103-50532006000500019.